The Physical Modelling of Two Phase Releases following the Sudden Failure of Pressurised Vessels

P. F. Nolan, N. R. Hardy, and G. N. Pettitt

*Fire and Explosion Research Group, Department of Chemical Engineering, South Bank Polytechnic, 103 Borough Road, London SE1 OAA, England.
†Technica Ltd., Lynton House, 7/12 Tavistock Square, London WC1 9LT, England.
‡Technica Inc., 355 E. Campus Blvd., Suite #170, Columbus, Ohio 43235.

ABSTRACT

Small scale experimental work involving the sudden and total failure of vessels containing pressurised liquids has led to the generation of information and data concerning the two phase releases produced. Vessel failure is simulated using two experimental techniques and the importance of "failure mode" observed. Experimental Data is presented, trends within the releases are described and some simple empirical expressions are derived. The work has led to the development of unique measurement systems that can be applied to larger scale experiments with ease.

INTRODUCTION

The use of pressure to store low boiling point materials as liquids is widespread and common throughout modern industry. The materials stored can be flammable or toxic (or both); they are stored at ambient temperatures, using their own vapour pressure to hold the material in the liquid phase. Pressure is maintained by the tensile strength of the vessel walls against the pressure exerted by the stored material. Releases from such vessels have occurred with disastrous consequences (e.g. [1], [2]).

This small scale work simulates catastrophic (sudden and total) failure of such vessels whereby the surface of the stored material will be instantly reduced to atmospheric pressure and the pressure decrease is transmitted through the material at the speed of sound. As depressurisation occurs, the thermodynamic equilibrium changes. In order to regain an equilibrium state some of the liquid will "flash boil" to vapour. The cooling of the remaining liquid to its normal boiling point at atmospheric pressure provides the latent heat of vaporisation necessary to achieve this. The flashed vapour will continue to expand until its pressure decreases to atmospheric. This will cause violent motion within the remaining liquid, the

expanding vapour bubbles causing it to break up. This action will result in some of the remaining liquid forming droplets that are entrained into the expanding vapour and carried away from the vessel.

As products of the two-phase release move away from the vessel three distinct parts can be discerned: the flashed and expanding vapour, the entrained droplets and the remaining body of liquid that has not been broken up. Such releases of flammable or toxic materials into the surrounding environment would be hazardous to life and, in the case of flammable releases, to property. The extent of this hazard will depend upon the thermodynamic, flammable and/or toxic properties of the material involved.

VESSEL FAILURE MODE

While it was not the intention of the study team to perform a detailed analysis of the mechanics of vessel failure it was appreciated at an early stage in the work that the range of possible scenarios is best envisaged as a spectrum with two extremes:

> [1] **Ductile Fracture** - an example would be the "tear" occurring as a vessel fails after long exposure to an impinging flame, relatively few large pieces yielded (sometimes there may be only one, much distorted, piece).
>
> [2] **Brittle Fracture** - the type of failure exhibited by glass or cast iron, numerous fragments of varying size being evolved.

The two experimental rigs used to simulate vessel failure in this work have been designed with the intention of representing "ductile" and "brittle" failure modes respectively.

Experimental Method #1.
This involved the use of aluminium spherical vessels of volume 6.8×10^{-4} m^3 and 8.5×10^{-5} m^3, held together as two hemispheres under pneumatic pressure, [3]. The vessel was filled to various levels with Refrigerant 11 (R-11) or Refrigerant 114 (R-114) used as the model material. Catastrophic failure was simulated, at various internal pressures and fill levels, by reversing the pneumatic cylinders, thus pulling the hemispheres apart. This event was recorded using high speed cine film (up to 1000 fps) and found, in summary, to consist of successive pulses of almost planar, radially expanding toroidal jet, perpendicular to the direction of the movement of the vessel halves.

Experimental Method #2.
Vessel failure was simulated through the destruction of spherical glass vessels, [4], containing R-11, R-114 and R-113. The model materials were again internally heated with failure being effected by mechanical impact (the impingement of a diamond tipped hammer) at a point along the horizontal axis of the vessel. This resulted in an initial escape from the part of the vessel walls surrounding the vapour phase (of a non-full vessel) suggesting crack propagation occurs more rapidly over this area. This was put down to a damping effect of the induced shockwave by the liquid layer and filmed evidence was supported by the fact that the vessel fragments from the vapour layer were smaller than those from that of the liquid. Another effect of this phenomenon was that at higher initial pressure, as the vessel failed, a larger proportion of the release was directed upwards and the cloud moved at higher speeds vertically than horizontally outwards.

It is not possible, or indeed desirable, to present all the results generated here. Therefore, unless otherwise stated, the results quoted will be those recorded using R-11, with a 50% fill in the relevant vessel with initial vessel pressure being the parameter focussed upon.

Similarly a detailed description of the measurement systems used will not be provided, this can be obtained from the authors' previous work ([3], [4], [5], [6]).

VESSEL OPENING CHARACTERISTICS

Information regarding vessel opening was obtained through filming for both pieces of apparatus but, because of the experimental differences, is expressed differently.

Experimental Method #1.
The area (A) available to the material in the vessel was found to be a linear function of time such that:

Large Vessel (6.8×10^{-4} m^3)	$A_L = 0.122\ t$
Small Vessel (8.5×10^{-5} m^3)	$A_S = 0.051\ t$

Where t is in seconds and A in m^2.

Experimental Method #2.
Opening time, the time at which the vessel is considered fully failed and not to hinder the release further, was observed to be a function of pressure and, to a lesser extent, fill level (see the above discussion on failure mode for Exp. #2). Table 1 presents the results from a series of experiments where only initial pressure was varied.

Table 1.

INITIAL INTERNAL PRESSURE (kPa)	OPENING TIME (ms)
45	18
95	8
140	6
172	4
206	<2
296	<2
410	<2
471	<1
570	<1

The development of expressions to define opening time from the above results is hampered by the somewhat arbitrary determination of the point at which the vessel is to be considered "fully open".

In summary the filmed overall release durations from both experiments can be expressed:

Experimental Method #1: Duration 0.2 - 0.3 s
Experimental Method #2: Duration 0.1 - 0.2 s

It becomes apparent that the slower vessel opening rate of Experimental Method #1 has a considerable effect on the release formed subsequent to failure.

RELEASE VELOCITY MEASUREMENTS

The velocity of the overall release (aerosol) has been measured for both experimental rigs using high speed cine film. Here, again the different techniques for failing the experimental vessel strongly characterise the results, consider figure 1 of mean exit velocity with initial pressure:

Figure 1.

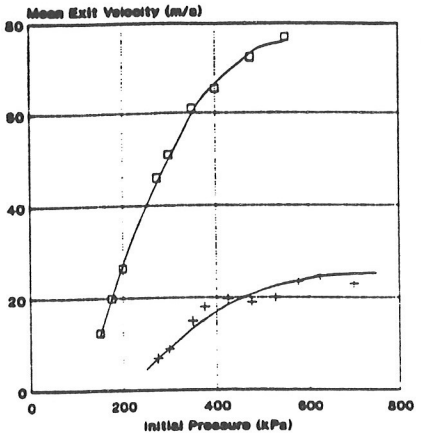

Experimental Method #1

The exit velocity was recorded with time over the entire release "circumference" over a range of pressures and a characteristic decay emerged, see figure 2 below:

Figure 2.

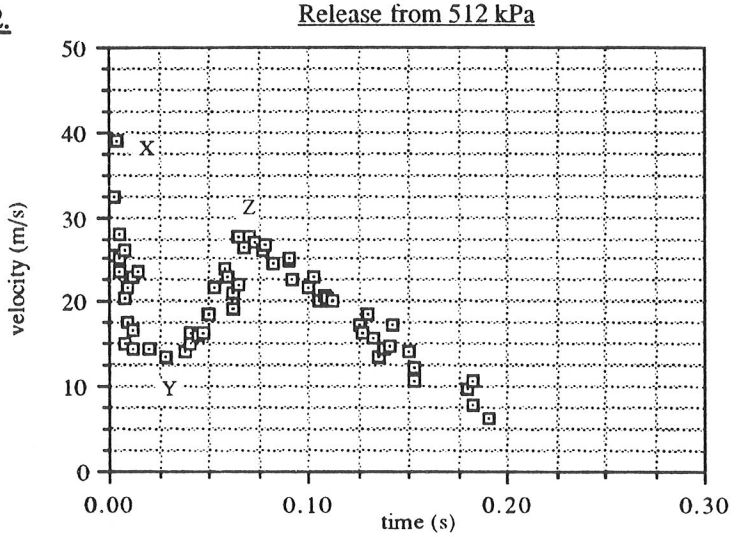

Curves of this type can be explained if it is assumed that, for this experimental rig, there is a slight delay in the onset of flashing (Z). The flashing is preceded by a high velocity vapour expansion, (X - Y), which, while entraining some liquid droplets, originates from the vapour layer of the vessel.

There are complex effects involved here and a full appreciation of events must incorporate an understanding of the variation of the number and size of droplets

generated with time. Results subsequently presented show that both the number and size of droplets around point Y on figure 2 is characteristically low, a small fraction of the initial mass of liquid held in the vessel. This has enabled development of a simple empirical expression to describe exit velocity (u) with time (t) as a function of initial pressure (P):

$$u = (0.014P - 14.35) - t(56.44 - 0.148P - 7.15x10^{-4}P^2)$$

Where: u is in m/s
t is in s
P is in kPa

This produces results:

Figure 3.

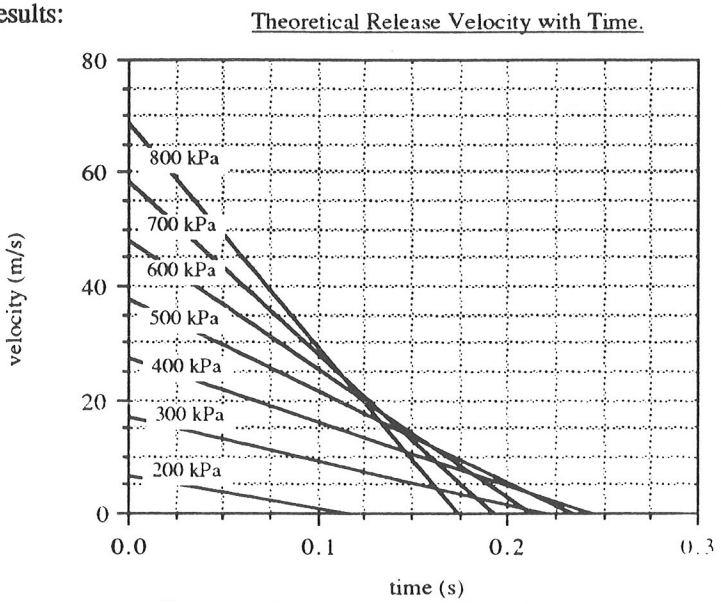

This relationship applies only to droplet velocities and vapour is likely to be moving more rapidly.

Experimental Method #2

Aerosol cloud front velocity measurements for this apparatus, by necessity, concentrated on the decay of velocity with distance, see figure 4.

Figure 4.

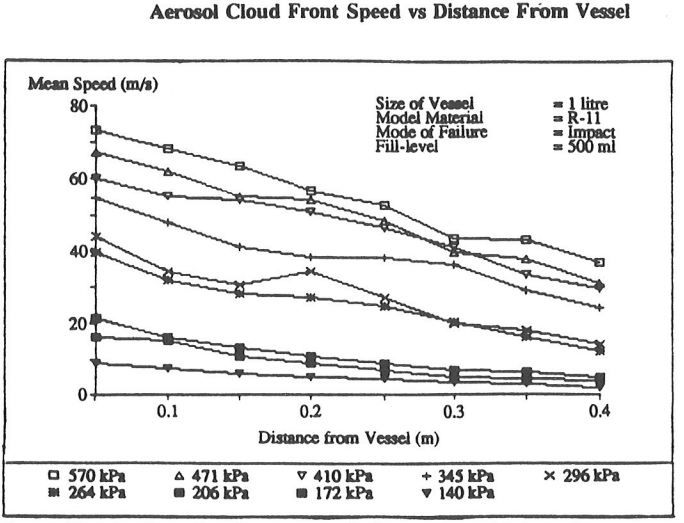

Extrapolation of this data back to r = 0 (vessel wall location) has led to the following relationship to describe mean exit velocity (u) with internal pressure (P):

$$u = -40.28 + 4.08\times10^{-1}P - 3.55\times10^{-4}P^2$$

Where u is in m/s and P in kPa.

Results from this expression were compared with those from the general expression for an isentropic expansion [7]. For an expansion from initial condition, 1, to some final condition, 2, (which may be atmospheric or greater) the initial front velocity is given by:

$$\tfrac{1}{2}u^2 = h_{f1} - [Xh_{fg2} + h_{f2}] - V_1(P_1 - P_a) + V_2(P_2 - P_a)$$

Where: u = Expansion Velocity
h = Enthalpy
X = Quality
V = Specific Volume
P = Pressure
$_f$ and $_g$ refer to liquid and vapour phases
$_1$, $_2$ and $_a$ refer to initial, final and ambient conditions.

Table 2 below shows a comparison between the exit speeds, i.e. at the beginning of the expansion, established from both experiment and theory for various internal pressures using a 50% fill-level of Refrigerant-11 in a 1×10^{-3} m^3 vessel. The results

indicate that the theoretical calculations overestimate the exit speed found by experiment by a value of approximately 30 m/s. In their experiments, Schmidli et al., [7], also found that the actual experimental values of expansion speed were overestimated by the theoretical model. They suggested that this is probably because the expansion speed is lowered due to conduction/convection processes during bubble growth.

Table 2 Exit Speed vs Internal Pressure

Internal Pressure (kPa)	Experimental Exit Speed (m/s)	Theoretical Exit Speed (m/s)
140	11	42.0
172	19	50.6
206	26	60.6
264	44	71.8
296	51	78.9
345	60	86.7
410	66	96.7
471	72	104.3
570	78	111.2

INTERNAL PRESSURE DECAY

The delay in the onset of flashing predicted after observation of the records of velocity decay recorded for experimental method #1 is supported by examination of the internal pressure histories recorded by an internally mounted transducer in one vessel "hemisphere" mounted on that rig; see figure 5, over:

Figure 5.

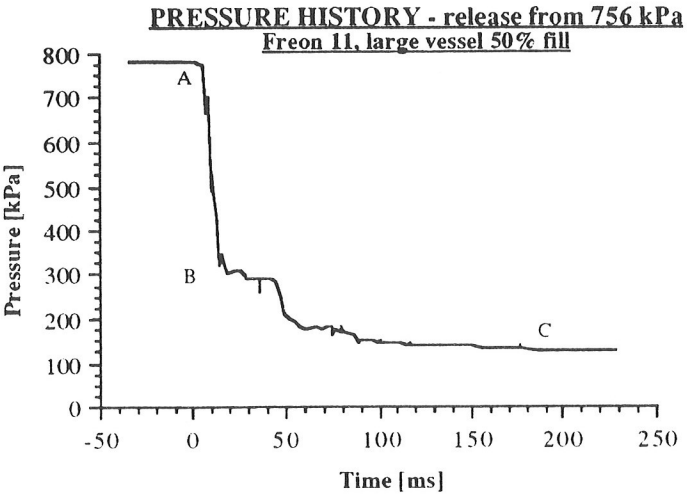

To aid explanation of the observed phenomena figure 5 has been labelled A, B and C, the decay is discussed below:

A — Release pressure, moment of simulated failure.

A - B — Rapid pressure decay due to vapour expansion.

B — Sudden transition to the "slower" flashing process which dominates recorded pressure.

B - C — A slower pressure decay during the flashing process, gradually settling down to atmospheric pressure.

This interpretation of results provides a likely explanation to the irregularities in figure 5 and similar traces - [i] The spikes during the initial, vapour related, decay are due to the pressure wave reverberation within the vessel, disturbing an otherwise relatively smooth decay (expansion); [ii] The flashing process is recorded as more turbulent because the nature of the process involves the transducer getting "bombarded" with liquid, this continues, with declining vigour, until equalisation.

MODE OF NUCLEATION

It was appreciated that there are two possible boiling regimes for the above experiments:

> [1] **Heterogeneous Nucleation** or nucleate boiling, where bubble formation occurs at the liquid / solid (e.g. vessel wall) interface, at "nucleation sites".
>
> [2] **Homogeneous Nucleation** occurs in the absence of, or without, nucleation sites such that normal flashing is suppressed and a metastable superheated liquid results. A depressurisation of this type could not be continued indefinitely - eventually the reduced thermodynamic limit of superheat would be reached and vapour formed in the bulk liquid. This "nucleation" occurs over a very short period (~μs) and results in a violent shock wave.

The shock wave mentioned in [2] above would manifest itself as a sharp increase in pressure on pressure records of the type presented above. That a "spike" does not appear supports the case for assuming a heterogeneous mode of nucleation in the described experiments.

Evidence of the occurrence of homogeneous nucleation in accident investigations is rare and some workers (e.g. [8]) have had difficulty generating results to support its occurring experimentally. Thermodynamic arguments to further support the nucleate boiling scenario have been advanced in previous work by one of the authors of this paper [3].

DROPLET CHARACTERISTICS

The recording of droplet characteristics was achieved using two separate pieces of equipment:

> [1] The use of a high speed camera, capable of filming at rates of up to 10,000 fps (40,000 with ¼ framing) in conjunction with a 10 Watt pulsed (synchronised) copper vapour laser and an industrial borescope.
>
> [2] A laser diffraction unit with operating range 0 - 1800 μm and dedicated particle sizing software.

The high speed cine work provided more detailed information about the releases,

but took longer to set up and analyse; the laser diffraction unit proved reliable for illustrating overall trends.

Droplet diameters reported, unless otherwise stated, are Sauter mean values, this is described as follows:

$$d_s = \frac{\sum n_0 d_0^3}{\sum n_0 d_0^2}$$

i.e. it is the ratio of the total volume to the total surface area. Hence, it is more representative of the total volume of liquid with respect to the number of droplets. For example, if there are two droplets of vastly different diameter, the arithmetic mean diameter will simply be the average diameter of the two droplets. The total volume based on this diameter and the number of droplets will be less than the actual volume. However, the Sauter mean diameter will be closer to the diameter of the larger droplet and generate the correct total volume, with respect to the number of droplets.

It is important to appreciate the complexity of such releases - for instance the combined effects of gravity (both trajectory "skew" and "rainout"), evaporation, and recording window location conspire to make the results more qualitative than quantitative. It becomes apparent that any droplet size distribution has both spatial (location specific) and temporal (time specific) components. The releases generated by the two experimental set-ups are effectively two and three dimensional respectively.

Analysis of the complete data set is ongoing.

Experimental Method #1

The trends illustrated by a series of experiments using both measurement systems are described below:

[1] Figure 6, over, is a typical plot of showing the number of droplets recorded with time at a point 0.65m away from the vessel centre.

Figure 6.

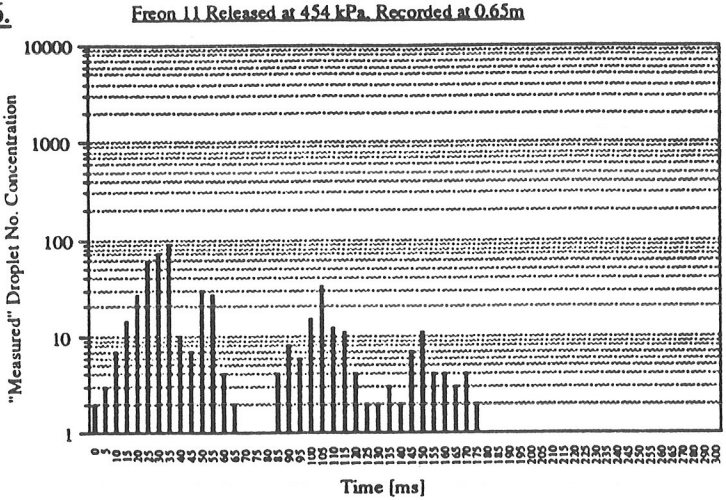

The two waves of droplets demonstrate agreement with earlier results (exit velocity measurement and pressure histories) in that the vapour expansion is followed by a distinct flashing process.

[2] The number of droplets observed decreased with distance away from the vessel due to evaporative, rainout and gravity skew effects (all results were taken horizontally away from the vessel) and the smaller relative size of the recording window.

[3] Size Distribution - detailed analysis of one run is presented (figures 7 & 8) and the distribution of droplet size for both phases has been characterised as log normal.

Figure 7.

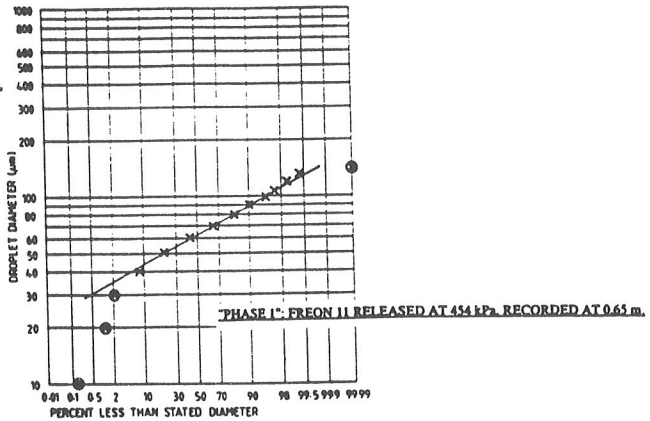

Figure 8.

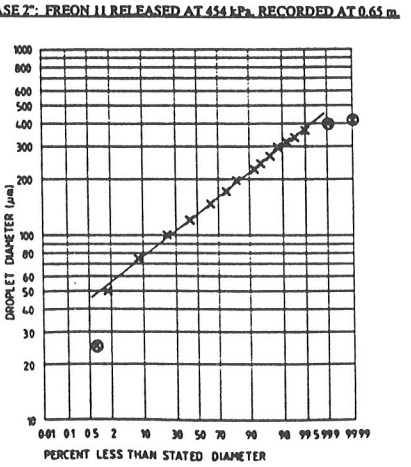

[4] Droplet size increases with time - this was expected, exit velocity has been shown to decay and the Weber No. [9] which is used to determine the stability of liquid jets, contains a velocity term:

$$N_{We} = \frac{\rho_g u^2 d}{\sigma}$$

Where: ρ_g = External gas density
u = Velocity of jet with respect to gas
d = Critical length dimension
σ = Surface tension

There are accepted "critical values" for the Weber No. and for a liquid jet of the type examined here a range is defined (12 - 30) above which "break-up "will occur. There is difficulty associated with determining critical Weber No. values for the experiments conducted because much of the data was obtained after the release had "broken-up"; and that gathered during "break-up" was not easily quantifiable. It was preferred to back calculate (knowing the mean exit velocity / pressure relationship, values for the density of air, and the surface tension / pressure relationship for R-11) enabling the calculation of the "maximum stable droplet diameter", see figure 9.

Figure 9.

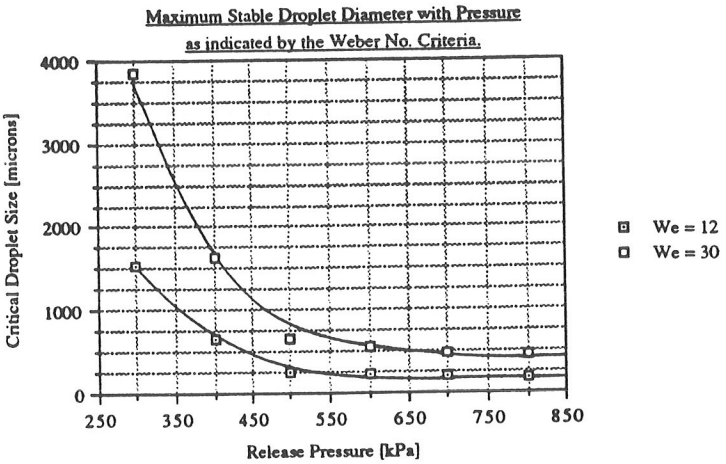

Comparison of these calculated values with mean droplet diameter data indicates that the N_{We} critical range can be reduced in the context of this work to between 20 and 30.

[5] Using the laser diffraction unit a decrease in droplet size was found with increased internal pressure, see figure 10.

Figure 10.

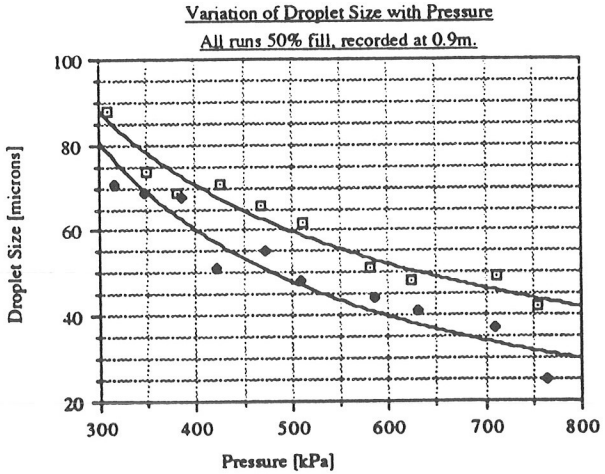

Experimental Method #2

The copper vapour laser photographic system proved extremely effective in the determination of droplet sizes, velocities, trajectories and concentrations and only results from this system will be presented for this experimental apparatus. Again a variety of trends become apparent:

[1] Figure 11 illustrates the droplet number changes with time. The droplet concentration rapidly increases to its peak value at 15 ms and then decays to zero with the exception of a second peak at about 26ms. This could be as a result of the phenomenon previously described for experimental rig #1 though the effect is less distinct.

Figure 11.

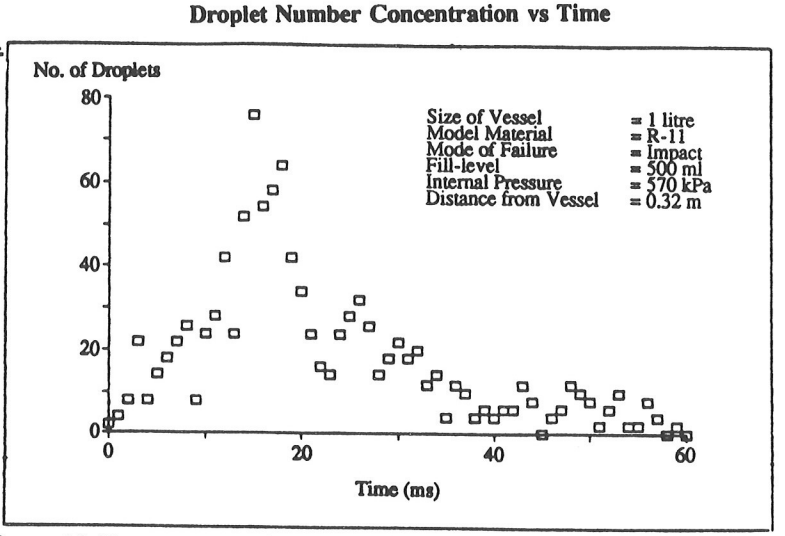

[12] Figure 12 illustrates a typical example of droplet size distribution.

Figure 12.

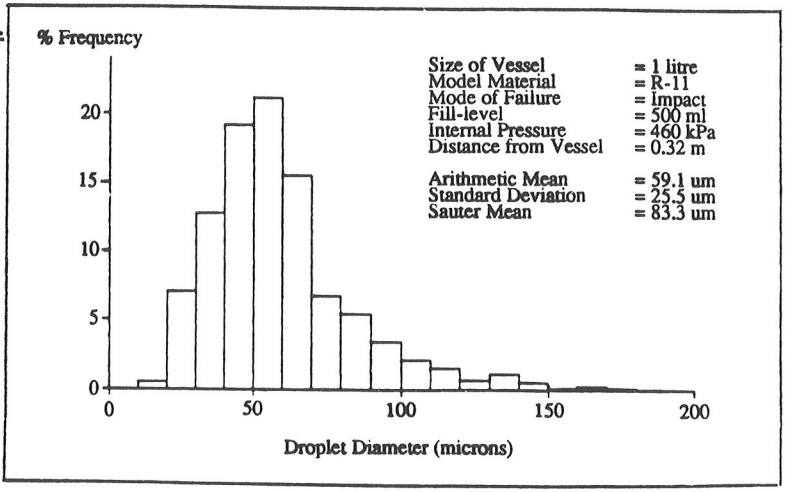

When the complete data set is examined the results indicate that droplets are distributed over a greater size range in releases at lower internal pressures (superheats) and higher fill-levels and that a log normal distribution again characterises results.

[3] Figure 13 indicates the variation of mean droplet diameter with distance, as the droplets are driven away from the vessel. The graph indicates that, for constant initial conditions, the mean droplet size decreases as the droplets move away from the vessel, quantification is again complicated by effects described earlier (expt. #1). In addition, at distances close to the vessel, (i.e. 0.16 and 0.22m), droplets are seen to break-up.

Figure 13.

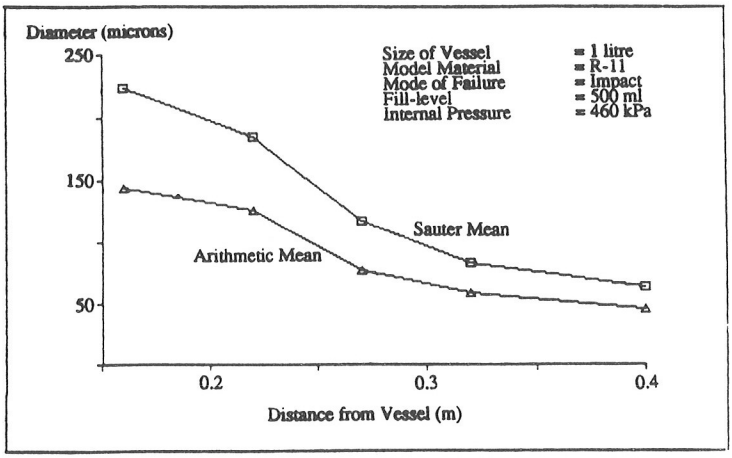

[4] Figure 14 shows that vessel fill-level influences the droplet size. The graph shows how the mean droplet size increases with fill-level.

Figure 14.

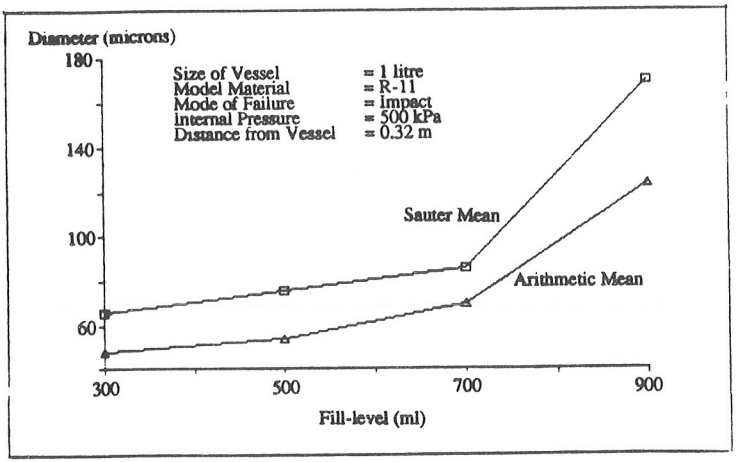

[5] Figures 15, 16 and 17 indicate how droplet size is also influenced by the internal pressure. All the graphs show that by increasing the internal pressure and

keeping all the other variables constant, the mean droplet size will decrease. Figures 15 and 17 also show that there is similarity between the results using Refrigerant-11 and Refrigerant-114 for similar initial conditions.

Figure 15.

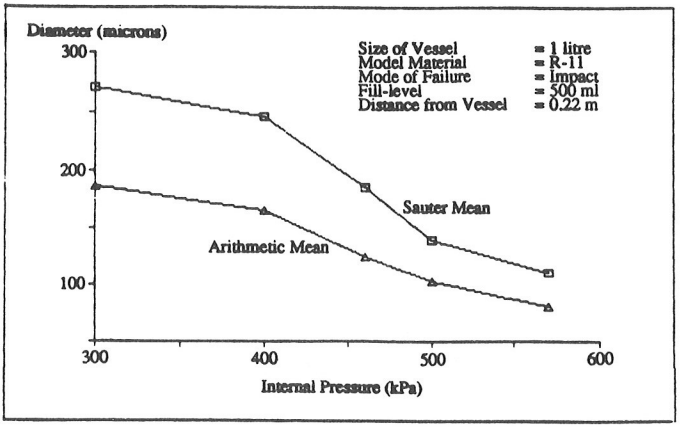

Figure 16.

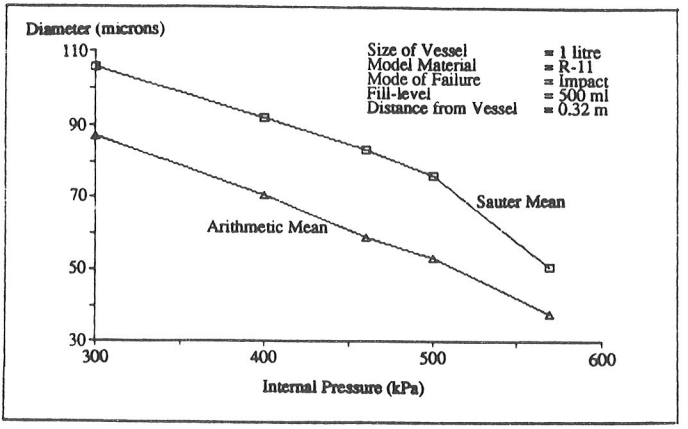

Figure 17.

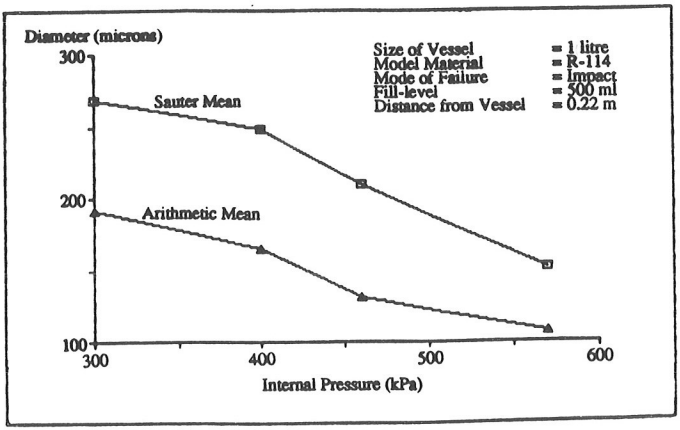

[6] Figures 18, 19 and 20 show how the graphs of droplet speed against time vary with internal pressure, fill-level and distance from the vessel respectively. Figure 18 indicates that droplet speeds increase with greater internal pressures. Figure 19 shows that the mean droplet speed decreases less rapidly as the fill-level is increased. Figure 20 indicates that droplets decelerate as they move away from the vessel.

Figure 18.

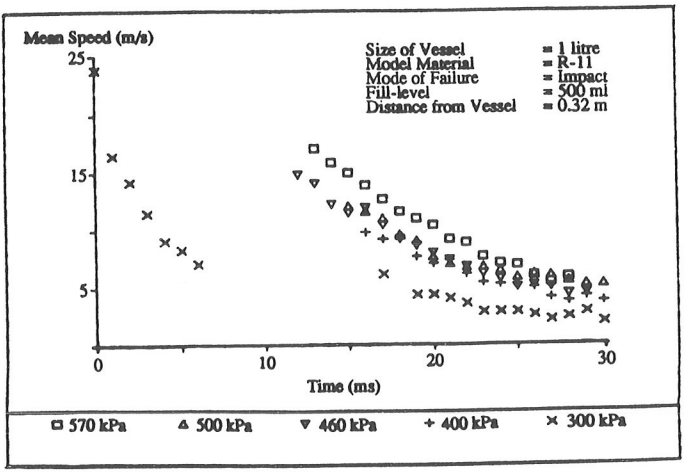

Figure 19.

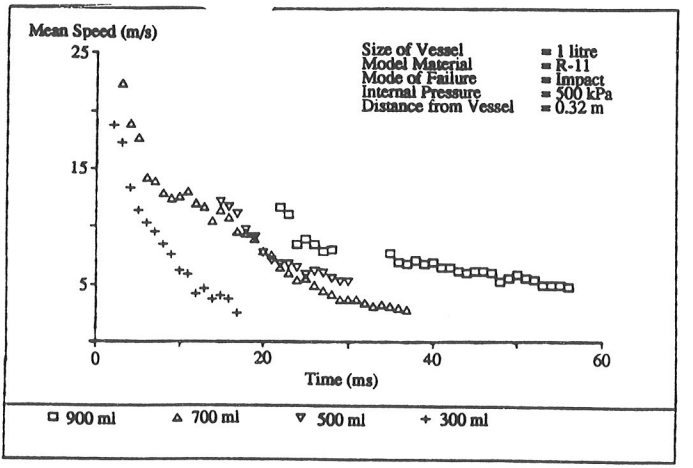

Figure 20.

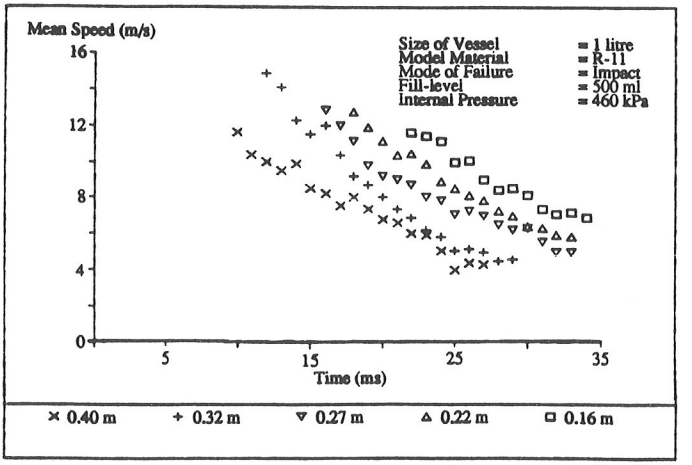

Results of individual aerosol droplets have also shown that some distance out, as the velocities of the droplets decrease, the speed of any given droplet becomes a function of its size at any point in time and space, i.e. the larger the droplet, the greater its speed. Figure 21 plots droplet velocity against droplet diameter.

Figure 21.

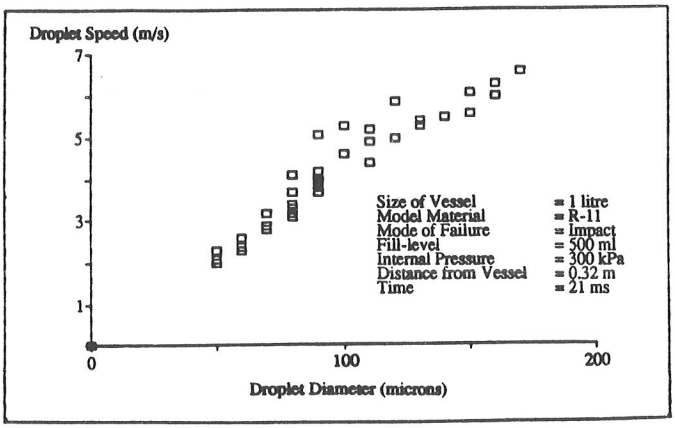

[7] High speed cine films of the droplet fronts provide an indication of their trajectories. At the beginning of a release, the droplets are source-driven and are propelled radially away from their original position. With increased time after failure the droplets begin to lose speed, turbulent effects cause the droplets to move in other directions and the effect of gravity gradually becomes more pronounced.

DISCUSSION

Both experimental rigs have been shown to generate repeatable results which characterise the two-phase releases generated. The "failure mode" is shown to strongly characterise the releases and comparison of the two data sets illustrates considerable differences.

It is generally appreciated that the value of work of this type hinges on the requirement of the experimental technique to have all the significant characteristics of a real system reproduced to scale (geometrically similar) and to satisfy material and design restrictions (kinematic and dynamic similitude). Work is being conducted using simple dimensional analysis and the Buckingham Pi Theorem to both introduce physical properties to the empirical equations generated by experiment and to assess the degree of similarity exhibited by systems of this type in terms of relevant dimensionless groups (eg. Reynolds No., Weber No.). Initial results are encouraging but the situation is complicated by the lack of relevant data at larger scales.

The measurement systems evolved during the course of this work have proved

successful and have applications both at larger experimental scales and outside this field.

ACKNOWLEDGEMENTS

The authors would like to thank the Technica Group, British Gas PLC and the (UK) Ministry of Defence for their independent support.

REFERENCES

[1] C.M.Pieterson, C.Cendejas Huerta, "Analysis of the LPG incident in San Juan Ixhuatapec, Mexico City, 19 November 1984", TNO, The Hague, 1984.

[2] H.Lonsdale, "Ammonia Tank Failure - South Africa", Ammonia Plant Safety Vol 17 (1975), A.I.Ch.E., pp 126 - 131.

[3] N.R.Hardy, "The Physical Modelling of Two Phase Releases Following the Sudden Failure of Pressurised Vessels" Ph.D. Thesis, CNAA, South Bank Polytechnic, London, UK, 1990.

[4] G.N.Pettitt "Characterisation of Two-Phase Releases" Ph.D. Thesis, CNAA, South Bank Polytechnic, London, UK, 1990.

[5] P.F.Nolan, G.N.Pettitt, N.R.Hardy, R.J.Bettis "Release Conditions Following Loss of Containment", J.Loss Prev. Process Ind., 1990, Vol 3 January.

[6] P.F.Nolan, G.N.Pettitt, N.R.Hardy, "The Characterization of Two-Phase Releases" Proceedings of Conference on Probabilistic Safety Assessment and Management (PSAM), University of California, Beverly Hilton, Beverly Hills, CA, 4 -7 February 1991.

[7] J.Schmidli, S.Banerjee, G.Yadigaroglu, "Experiments on Vapour / Aerosol and Pool Formation on Rupture of Vessels Containing Superheated Liquids", J.Loss Prev. Process Ind. 1990, Vol 3 January.

[8] J.D.Reed, "Containment of Leaks from Vessels Containing Liquified Gases With Particular Reference to Ammonia", First International Symposium on Loss Prevention & Safety Promotion in the Process Industries, pp 191 - 197, Amsterdam, Netherlands, 1974.

[9] C.Weber, Ziet fur Angew. Math., Vol 11, 106, 1938.